

## Shining Light on Non-Chemical Steps in Protein Catalysis

- Combining CD and fluorescence spectroscopy (Chirascan V100 with fluorescence accessory) with stopped-flow kinetics (Stopped-flow accessory and SX20) is a powerful approach to elucidating enzymatic pathways
- Stopped-flow based on rapid fluorescence kinetics and near-UV CD in presence of viscogens reveals the role of local unfolding in the redox cycle of peroxiredoxin Tsa1 and allows assignment of kinetic phase

Data courtesy of Sophie Rahuel-Clermont, Ph.D., Biophysics and Structural Biology Core Facility, Université de Lorraine [1].

### Summary

Biochemical reactions in enzymatic pathways are commonly characterised by spectroscopically monitoring participating educts or products—the characterisation of non-chemical steps is challenging and less often pursued. However, a careful experimental strategy making use of orthogonal spectroscopic signals can overcome this challenge.

As an example, the redox cycle (Figure 1) of the peroxiredoxin Tsa1 from *S. cerevisiae*, which provides protection against oxidative stress and is involved in cell redox signalling, was explored using stopped-flow spectroscopy based on both intrinsic fluorescence and near-UV CD signals [1]. This provided direct information about the kinetics of the conformational transition and sulfinylation of the protein, which is critical for understanding and predicting the hyperoxidation sensitivity of Tsa1 and similar enzymes [2].

Ultimately, results of this study benefit understanding of human peroxiredoxins as well. These have, for example, the potential to serve as clinical targets for cancer therapies, as their hyperoxidation is linked to cancer stem cell stemness [3].

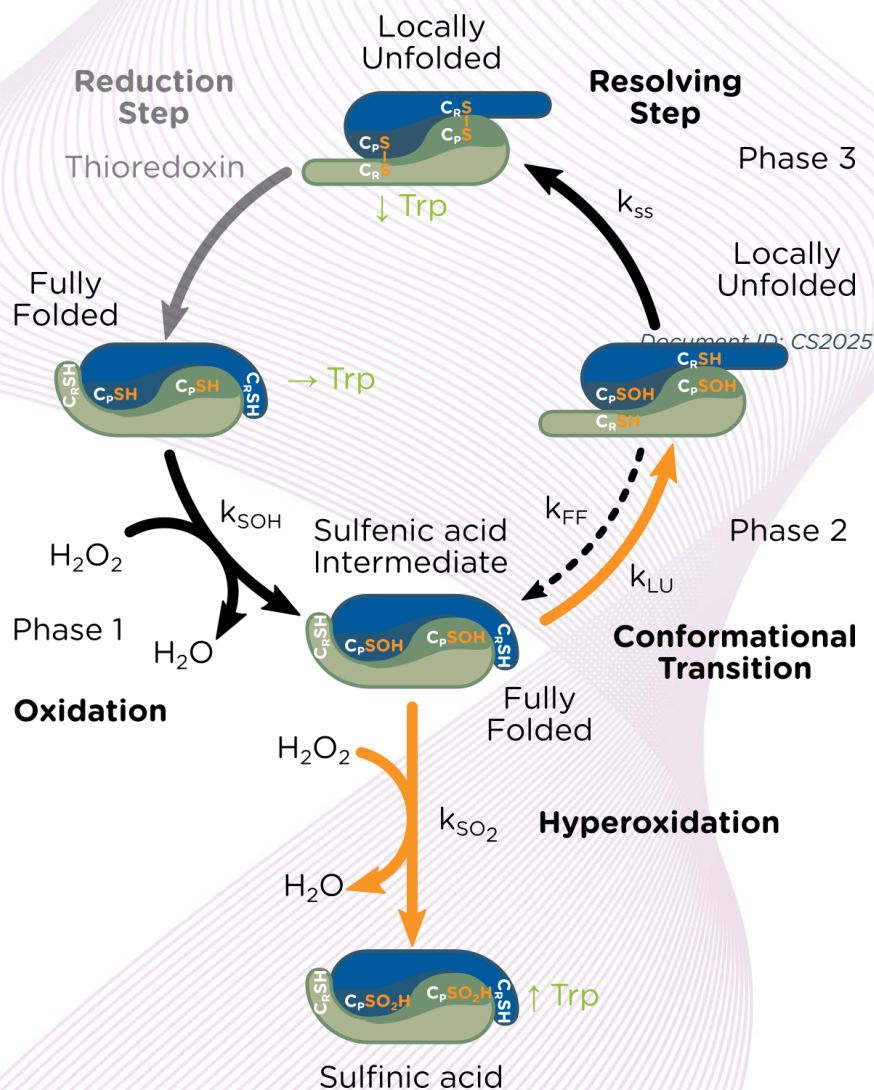


**Figure 1:** Catalytic cycle of Tsa1. Different states of the enzyme can be discerned by their different responses of intrinsic Trp fluorescence (↓ low, → medium, ↑ high). Adapted from [1].

## Method

**Circular Dichroism.** All data shown were obtained with a Chirascan V100 system. Far- and near-UV CD spectra were obtained using pathlengths of 0.1 mm and 10 mm, respectively. Tsa1 was used at 50  $\mu\text{M}$  in 10 mM sodium phosphate buffer, pH 7, containing 100 mM NaF. CD spectra are averages of 3 repeat scans at a step size of 1 nm.

Near-UV CD kinetics were obtained using a Chirascan SF.3 stopped-flow accessory coupled to the system at a bandwidth of 4 nm and averaging 50 measurements.

**Fluorescence Stopped-Flow.** Kinetics were monitored by fluorescence on an Applied Photophysics SX20 instrument equipped with a 5  $\mu\text{L}$  cell. Equal volumes of Tsa1 and  $\text{H}_2\text{O}_2$  were mixed while exciting at 295 nm and collecting fluorescence emission above 320 nm. For further experimental details, refer to [1].

## Results & Discussion

While previous studies have elucidated the kinetics of sulfenic acid formation ( $k_{\text{SOH}}$ ) and hyperoxidation ( $k_{\text{SO}_2}$ ), details about the conformational transition of Tsa1 ( $k_{\text{FF}}$ ,  $k_{\text{LU}}$ ) have been sparse because characterising non-chemical steps of a catalytic process is difficult. However, with the right tools and an elaborate experimental strategy, it is feasible; accordingly, the study outlined in this Application Note provided direct information about the kinetics of this transition for a better understanding of the origin of peroxiredoxin sulfinylation sensitivity.

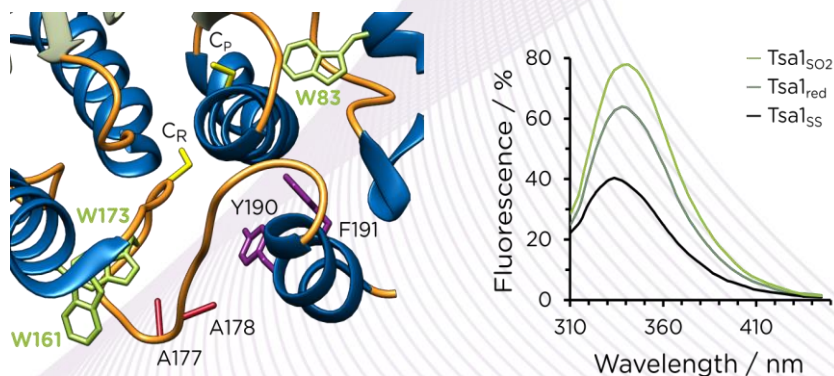


**Figure 2:** The active site of Tsa1 contains multiple tryptophan residues (left, green). Therefore, the fluorescence response of the enzyme is sensitive to its redox state (right).

**Intrinsic Trp Fluorescence** can resolve catalytic steps. Tsa1 contains three Trp residues that show a fluorescence emission dependency on the redox state of the enzyme (**Figure 2**), so the reaction of Tsa1 with  $\text{H}_2\text{O}_2$  under single turnover conditions (in absence of thioredoxin) was followed by fluorescence.

By this approach, three kinetic phases were identified (**Figure 3**, left). The first phase rate constant showed linear dependency on  $\text{H}_2\text{O}_2$  concentration and was shown to reflect the irreversible attack of  $\text{H}_2\text{O}_2$  by the catalytic Cys C<sub>P</sub>. Preliminary measurements indicated that phases 2 and 3 were monomolecular events not related to hyperoxidation and, therefore, had to correspond to later mechanistic steps in the redox cycle.

**Identifying conformational changes using viscogens.** Identity of phase 2 was distinguished from chemical steps of the catalytic cycle by stopped-flow experiments in presence of saccharose, which acts as a viscogen, slowing down conformational changes of proteins. As only phase 2 slowed down under these conditions (**Figure 3**, right), it can be deduced that this is likely a conformational transition of Tsa1.

A full picture using an orthogonal approach, **Stopped-Flow CD**. To further reveal the identity of phase 2, experiments were carried out by CD spectroscopy and near-UV CD stopped-flow. A mutant of Tsa1 was used in which residues Y190 and F191 (**Figure 2**, left, purple) are replaced by glycines. These substitutions destabilize the C-terminal  $\alpha$ -helix of the mutant, and, therefore let it adopt the locally unfolded conformation (see **Figure 1**). Comparison of far- and near-UV CD spectra between wild-type and mutant confirms that the secondary and tertiary structure of the mutant are virtually identical to those of the oxidised disulphide wild-type enzyme which is locked in the locally unfolded conformation (**Figure 4**).

The near-UV CD profile shows a large difference between the two states, which is most significant at around 270 nm. This wavelength was utilized in a near-UV CD stopped-flow experiment where the pre-steady state kinetics for the reaction between wild-type Tsa1 and  $\text{H}_2\text{O}_2$  was monitored. The kinetic rate constant obtained ( $k_{\text{LU}} = 54 \pm 2 \text{ s}^{-1}$ )

was highly similar to that from fluorescence measurements ( $k_{LU} = 64 \pm 2 \text{ s}^{-1}$ ) and therefore confirmed that phase 2 in the catalytic cycle of Tsa1 corresponds to the transition between fully folded and locally unfolded states.

Finally, successful assignment of phases 1 and 2 implies that phase 3 must reflect the final resolving step of the catalytic cycle in which cysteines  $C_P$  and  $C_R$  form a disulphide bond.

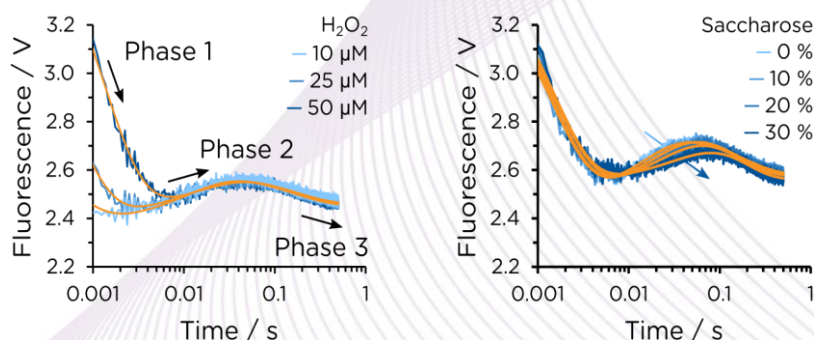


**Figure 3:** Fluorescence stopped-flow allows identification of three-exponential kinetics upon reaction of Tsa1 with  $\text{H}_2\text{O}_2$  (left). Phase 1 depends on  $\text{H}_2\text{O}_2$  concentration and was assigned to initial formation of  $C_P\text{-SOH}$ . Phase 2 is slowed down in the presence of a viscogen and thus corresponds to the conformational transition of Tsa1 (right).

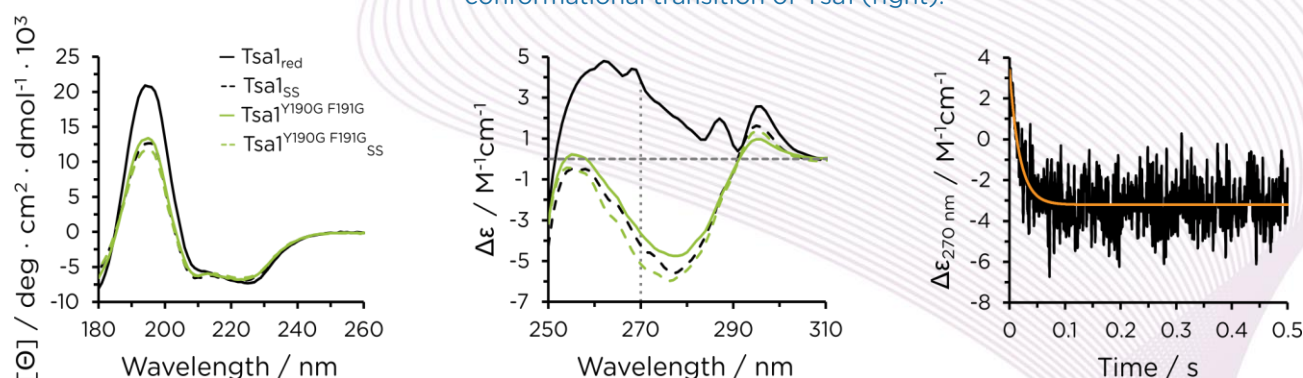


**Figure 4:** Far- (left) and near-UV CD spectra (middle) for reduced and oxidised states of wild-type Tsa1 and Tsa1 mutant Y190G F191G, and near-UV CD stopped-flow data for Tsa1 wild-type oxidation (right), confirming that phase 2 in the catalytic cycle of Tsa1 corresponds to its conformational transition between fully folded and locally unfolded states.

## Conclusion

Stopped-flow experiments using Applied Photophysics SX20 and Chirscan V100 SF.3 systems allow monitoring of different spectral properties including fluorescence, absorbance, and even far- and near-UV CD.

With these tools, the study outlined here established that the transition between fully folded and locally unfolded states of Tsa1, in its sulfenic acid form  $C_P\text{-SOH}$ , is not in rapid equilibrium as previously hypothesised, but almost irreversible ( $k_{FF} \sim 0 \text{ s}^{-1}$ ) and in direct competition with the hyperoxidation step.

## References

1. A. Kriznik, M. Libiad, H. Le Cordier, S. Boukhenouna, M. B. Toledano, and S. Rahucl-Clermont, 2020, *ACS Catal.*, 10, 3326–3339.
2. Z. A. Wood, L. B. Poole, and P. A. Karplus, 2003, *Sci.*, 300, 650–653.
3. Y. W. Son, M. G. Cheon, Y. Kim, and H. H. Jang, 2019, *Free Radic. Biol. Med.*, 134, 260–267.

© Applied Photophysics Limited, 2018. All rights reserved. Chirscan™ is a trademark of Applied Photophysics Limited. All other trademarks are the property of their respective owners.